NUCLEAR-STRUCTURE STUDIES USING PARTICLE-γ COINCIDENCES: PRESENT AND FUTURE

ESTUDIOS DE ESTRUCTURA NUCLEAR USANDO COINCIDENCIAS γ-PARTÍCULA: PRESENTE Y FUTURO.

Walter Reviol, Demetrios G. Sarantites

Department of Chemistry, Washington University, St. Louis, MO 63130, USA

(Recibido: Marzo/2015. Aceptado: Julio/2015)

Abstract

Reaction-channel selected γ-ray spectroscopy is a key method in nuclear-structure studies far from the β-stability valley. Examples of such experiments on both sides of the valley are discussed and some of the typical detector setups are introduced: the HPGe arrays Gammasphere and Gretina and the available suite of associated particle detectors. The use of stable and radioactive ion beams is covered (to some extend) as well. A sort of historical perspective is presented stating that the emphasis in nuclear-structure studies has shifted from proton-rich to neutron-rich nuclei.

Keywords: heavy-ion reactions, γ-ray spectroscopy, reaction-channel selection, Doppler correction.

Resumen

El método de selección de canales de reacción en espectroscopía de rayos γ ha sido clave en los estudios de estructura nuclear para núcleos lejos del valle de estabilidad β. Ejemplos de tales experimentos en ambos lados del valle de estabilidad son discutidos y se presentan algunos de los arreglos experimentales típicos: Gammasphere y

Walter Reviol: reviol@wustl.edu

Gretina, con detectores de Germanio hiperpuro, incluyendo un conjunto de detectores de partículas. Se presentan el uso de haces de iones estables y radioactivos, así como las perspectivas históricas de la estructura nuclear que han buscado la consistencia, desde los núcleos ricos en protones hasta los ricos en neutrones.

Palabras clave: reacciones de iones pesados, espectroscopía de rayos γ, selección de canales de reacción, correccción Doppler.

Introduction

The continuous development of 4π arrays of HPGe detectors over the last 25 years has led to large gains in both the γ-ray detection efficiency and resolving power, see Ref. [1]. The selectivity of these arrays can be enhanced considerably by using them in conjunction with dedicated particle detectors, called auxiliary detectors. The present paper focuses on coincident detection of heavy-ion reaction products and the de-excitation γ-rays of one or several of these products. The restriction made here is that only experiments with comparatively slow heavy-ion beams are discussed, namely with beam energies $E_{lab} < 10$ MeV per nucleon. The targets are typically thin metallic foils with a surface density of 1 mg/cm^2 or less. The velocities of the recoiling products can be as high as 10% of the vacuum speed of light, leading to appreciable Doppler shifts of the γ rays emitted from the nuclei in flight. The auxiliary detectors are designed to serve two purposes. (i) They provide the ability of selecting the reaction channel of interest, i.e., they help to identify which product emitted a certain γ-ray. (ii) They help to determine the recoil directions and velocity vectors and, thus, aid in the Doppler correction of the γ-ray energies. The velocities are essentially constant, due to the thin target, and this reduces the occurrence of Doppler-broadened line shapes, which are in most cases undesired.

The γ-spectroscopic information is of pivotal interest. It contains a large set of excited-state observables and features, which are listed hereafter.

- Spin, I (obtained from an angular distribution or correlation, see Sec. 2.2 of Ref. [2]);
- Parity, π (from the linear polarization [ibid.] or the balance of feeding and decay intensity after correcting for internal conversion);
- Lifetime, τ (from e.g. measurements using Doppler methods such as the DSA method, see Sec. 8.4 of Ref. [2]);
- Reduced quadrupole transition probability, $B(E2)$, see Sec. 2.3 of Ref. [2] (from τ); this quantity leads to the size of the quadrupole deformation of the nuclear shape, also called transition quadrupole moment;
- $B(E\lambda)$, $\lambda \geq 3$ (ibid.); this may lead to higher-order deformations, e.g., an octupole shape ($\lambda = 3$);
- Quadrupole moment (from static-moment measurements, see Sec. 3.3 of Ref. [2], or from multi-Coulomb-excitation sum rules, see Ref. [3]); it gives the size and sign of the quadrupole deformation;
- Magnetic moment [from the perturbed angular distribution or correlation of the magnetic type, see Sec. 9.2 of Ref. [2], or from the reduced magnetic transition probability, $B(M1)$]; it points to the nucleon configuration for the state of interest;
- Emission sequence and level pattern; it may indicate e.g. a rotational-like behavior of the nucleus [$I(I+1)$ dependence of the level energy, see Sec. 7.8 of Ref. [2]].

The above measurements work provided that the γ-ray spectra are clean and discrete lines are well resolved. However, as one departs from the β-stability valley there is an increasing fragmentation into various reaction channels and a "tag" is needed for the channel of interest, which is provided by an auxiliary detector. By the same token, collection of particle-γ coincidence data is especially important in regions of the nuclear chart far from stability.

It is not possible to cover in a short paper all relevant setups for particle-γ coincidence measurements. The examples presented are taken from the authors' surroundings: the focus is on the HPGe arrays Gammasphere and Gretina and the available suite of auxiliary devices. The auxiliary devices for Gammasphere include the Microball light-charged-particle detector [4], the Neutron Shell [5], the HERCULES evaporation-residue detector [6], and the CHICO heavy-ion counter [7]. Some of their respective successors have been used, as intended, in Gretina experiments, namely CHICO-2 [8] and the Phoswich Wall [9]. The latter two devices are yet not documented in the literature, and brief descriptions are in order.

CHICO-2 represents an array of 20 parallel-plate avalanche counters. It covers a similar range of angles as its predecessor, but provides a higher resolution of the azimuthal angle, ϕ, than that one ($\Delta\phi \sim 1^\circ$ vs. 9°). The improvement is due to changing the position-sensitive cathode board of Ref. [7]. The idea is further improving the Doppler-correction capability of the combined detector setup as well as permitting higher count rates. Probably the main application of the CHICO and CHICO-2 devices is multi-step Coulomb excitation, using "symmetric" target-projectile combinations, i.e., reaction partners with similar masses.

The Phoswich Wall is a highly pixelated (256-element) system of fast-plastic + CsI(Tl) detectors. The light from both scintillator layers is read out by 4 closely packed multi-anode phototubes of 64 elements each. The phoswich technique is used to separate the fast signal in the thin front detector (energy-loss signal, ΔE) from the slow signal in the thicker rear detector (energy signal, E). The ΔE-E measurement allows identification of particles and light ions by the atomic number. This adds to the "CsI(Tl)-inherent" particle-identification capability by pulse-shape discrimination, discussed in Ref. [4]. The solid-angle coverage of the Phoswich Wall is 1.5 π.

The Microball and the equivalent Hyball [10] CsI(Tl) 4π detector arrays have been used in both fusion-evaporation and binary-reaction experiments. In the latter case, however, the nucleon-transfer and Coulomb-exitation measurements were conducted in strongly inverse kinematics, i.e., with rather light targets and much heavier beams. For these reactions, the Phoswich Wall is the successor of Microball-type devices. Here, it has the same efficiency those devices have, but enhanced identification capabilities and a higher resolution of both the azimuthal angle and the polar angle with respect to the beam axis, θ ($\Delta\theta \sim \Delta\phi \sim 3^\circ$ for a pixel, but sub-pixel resolution is possible [9]).

From the above considerations, it is clear that each auxiliary detector is optimized for a different class of experiments and the physics studies being pursued. Often the detectors are complementary to one another. For instance, CHICO-2 is predestined for symmetric binary reactions, while strongly inverse-kinematic conditions suggest using the Phoswich Wall. There are also common requirements such as minimal impact on the performance of the γ-ray array (low-mass detector design, etc.) and large solid-angle coverage. In the following sections, the accessibility of nuclei far from stability is addressed, some typical experiments in both the proton-rich and neutron-rich regime of the nuclear chart are discussed, and finally a summary is presented.

Accessibility of nuclei far from stability

The two principal territories on the nuclear chart reach from the β-stability valley to either the proton or neutron dripline. An up-to-date representation of the chart is shown in Fig. 1 of Ref. [11]. For the nuclei in the proton-rich territory, both the ground- and excited-state properties are rather well known. Indicative of this progress is, e.g., the delineation of the proton dripline up to element 91. The neutron-rich regime is not only the wider of the two territories, but also the one that is less known. Just for comparison, the neutron dripline is established up to element 8. This lack of knowledge is due to the fact that the neutron-rich

region is hard to access by nuclear reactions. However, neutron-rich nuclei have a large discovery potential, even those that are close to stability.

Proton-rich nuclei are typically produced in heavy-ion induced fusion-evaporation reactions. The proton-rich compound nucleus subsequently emits neutrons or charged particles (protons, α particles, low-mass fragments) or undergoes fission. The yields of these channels depend on the mass region, but also on the compound-nucleus excitation energy and angular momentum. This reaction type has been the workhorse for exploring the proton-rich territory, but is of little use in neutron-rich studies. In recent years, projectile-fragmentation reactions [12] have been used to study certain properties of very proton-rich nuclei; they are in many cases an alternative to fusion-evaporation reactions.

Neutron-rich nuclei can be produced in various ways. Particularly useful are neutron-transfer reactions, induced and spontaneous fission, and again fragmentation reactions. The reach of suitable transfer reactions into the neutron-rich territory can be expanded by using neutron-rich rare-isotope beams made from some of the above products. Hence, in present days most transfer-reaction studies are using inverse kinematics, employing the variety of available beam species. Moreover, the steadily increasing availability of neutron-rich beams will also revitalize proton-transfer studies, as the location of proton states in neutron-rich nuclei is as topical as that of the neutron states [13].

Present-day rare-isotope beams have comparatively low intensities. Therefore, reactions are preferred where the cross section is high (in excess of 100 mb), in order to achieve the physics goals of such experiments within a reasonable amount of time. Under the experimental conditions introduced above (thin targets and beams with $E_{lab} < 10$ MeV per nucleon), Coulomb excitation and, to a lesser extent, one-nucleon transfer reactions are of current interest to the experimenters. These studies can be summarized as experiments with so-called re-accelerated beams.

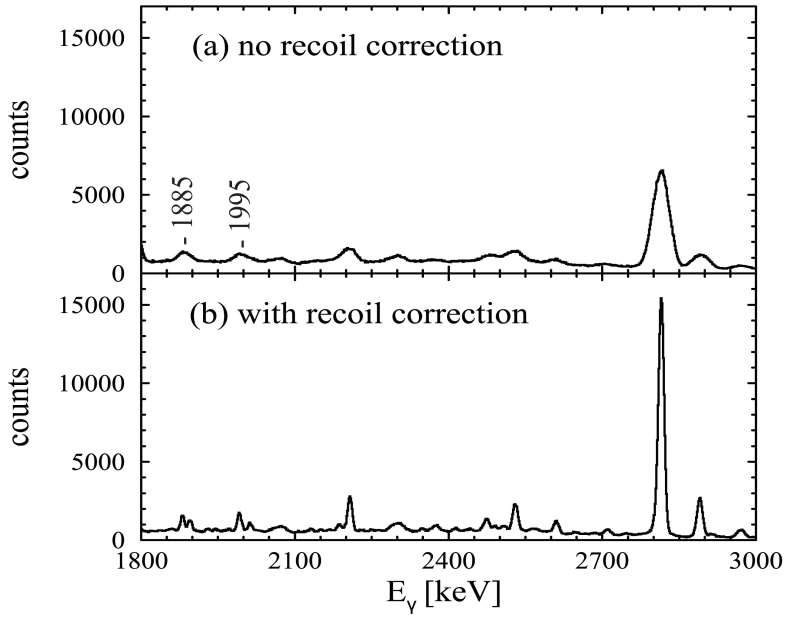

FIGURE 1. *Spectra gated on the 2αp channel and a transition in* ^{39}K *(E_γ = 757 keV) without (a) and with (b) a recoil Doppler correction. The figure is reproduced from Ref. [14].*

In-beam experiments in the proton-rich regime

The experiments discussed in this section deal exclusively with proton-rich nuclei produced in fusion-evaporation reactions. Among the themes and issues explored in these studies are superdeformation in the mass-40, 60, and 80 regions and properties of self-conjugate nuclei. Here, Gammasphere and the Microball have been the centerpieces of the setup.

In the study of ^{40}Ca, ^{28}Si(^{20}Ne,2α) and ^{24}Mg(^{24}Mg,2α) reactions were used, a superdeformed band was delineated, and its transition quadrupole moments were measured [15]. The Microball helped to select the 2α evaporation channel and "sharpen" the γ-ray spectra. Figure 1 shows an example for the improved Doppler correction in one of the experiments, namely for the ^{28}Si(^{20}Ne,2αp)^{39}K side channel. Panel (a) displays a γ-ray spectrum obtained after a Doppler correction with respect to the beam axis. Panel (b)

presents the corresponding spectrum for an event-by-event Doppler correction based on the recoil-velocity vector. Note that in this spectrum the peaks at around 1885 and 1995 keV are resolved into two doublets.

The Gammasphere + Microball setup has been combined with the Neutron Shell, particularly in experiments in the mass-60 region. For the study of proton-rich ^{54}Co, the ^{28}Si(^{32}S,αpn) reaction was used, requiring neutron-gating capabilities [16]. The detailed knowledge about the ^{54}Co level scheme helped to adjust certain parameters for shell-model calculations in the region of doubly-magic ^{56}Ni as well as constraining the intruder-configuration space for the high-lying superdeformed band structures found in neighboring nuclei.

Many of the mass-60 superdeformed structures have, at the band head, a proton-decay branch that competes with γ decay. This rather outstanding feature was originally discovered with the Microball. In a "case study" for ^{56}Ni (populated via 2α evaporation) [17], the Microball was augmented by a Si array. Here, it was demonstrated that the proton-energy spectrum in coincidence with superdeformed γ-ray transitions has a sharp low-energy peak, while the corresponding spectrum gated by a transition in the ^{55}Co daughter nucleus features the broad distribution one expects for the evaporation protons of a reaction side channel.

In another class of experiments, γ-ray spectroscopic studies in the actinide region have been performed. For fusion reactions in this region, fission dominates over the formation of evaporation residues. Therefore, a "tag" is required that helps to separate the γ rays of the residues from those of the fission products and other sources of background. One way to meet this requirement is to directly detect the residue nuclei by time-of-flight and pulse height with a device like HERCULES. This detector is due to its comparatively large polar-angle coverage suitable for very asymmetric normal-kinematic reactions, as these lead to broad,

forward peaked residue angular distributions. Indeed, the Th nuclei at around mass 220, having been in the focus of recent studies, could only be produced in such reactions.

Figure 2 shows a set of γ-ray spectra from an experiment with Gammasphere and HERCULES aimed at studying ^{219,220}Th [18]. The ^{219,220}Th nuclei are produced, respectively, in the ^{198}Pt(^{26}Mg,xn) $x = 5$ and 4 neutron-evaporation channels. The "raw" spectrum of Fig. 2 (a) is dominated by background from fission fragments, target X rays, contaminant peaks from inelastic neutron-scattering products, and Coulomb excitation. The spectrum of Fig. 2 (b) demonstrates the impact of residue gating: the peak-to-background ratio has improved by two orders of magnitude. The lines of interest, e.g., the 234-keV transition in ^{220}Th, "stick out" now. Figure 2 (c) shows a sample residue- and γ-gated spectrum for ^{220}Th; the gating transition is the 146-keV line. The studies in this region have revealed the onset of octupole collectivity near the $N = 126$ neutron closed shell. They also provide a clear picture of parity-doublet bands in odd-mass nuclei, see Ref. [19].

In-beam experiments in the neutron-rich regime

The experiments discussed in this section deal with heavy stable isotopes and neutron-rich nuclei. Here, the auxiliary detectors are CHICO and CHICO-2, the Microball and the Hyball, and the Phoswich Wall.

In a typical experiment with the Gammasphere-CHICO combination, inelastic excitation of ^{170}Er by a ^{238}U beam, at energies near the Coulomb barrier ($E_{lab} = 1358$ MeV), was studied [20]. The choice of the bombarding energy helped to populate target-nucleus levels at high excitation energy and spin, although the energy was "unsafe" for a standard Coulomb-excitation experiment [3]. By using thin target foils (~ 0.5 mg/cm^2), sharp γ-ray lines up to the highest-spin levels were observed. Both target- and projectile-like nuclei were detected,

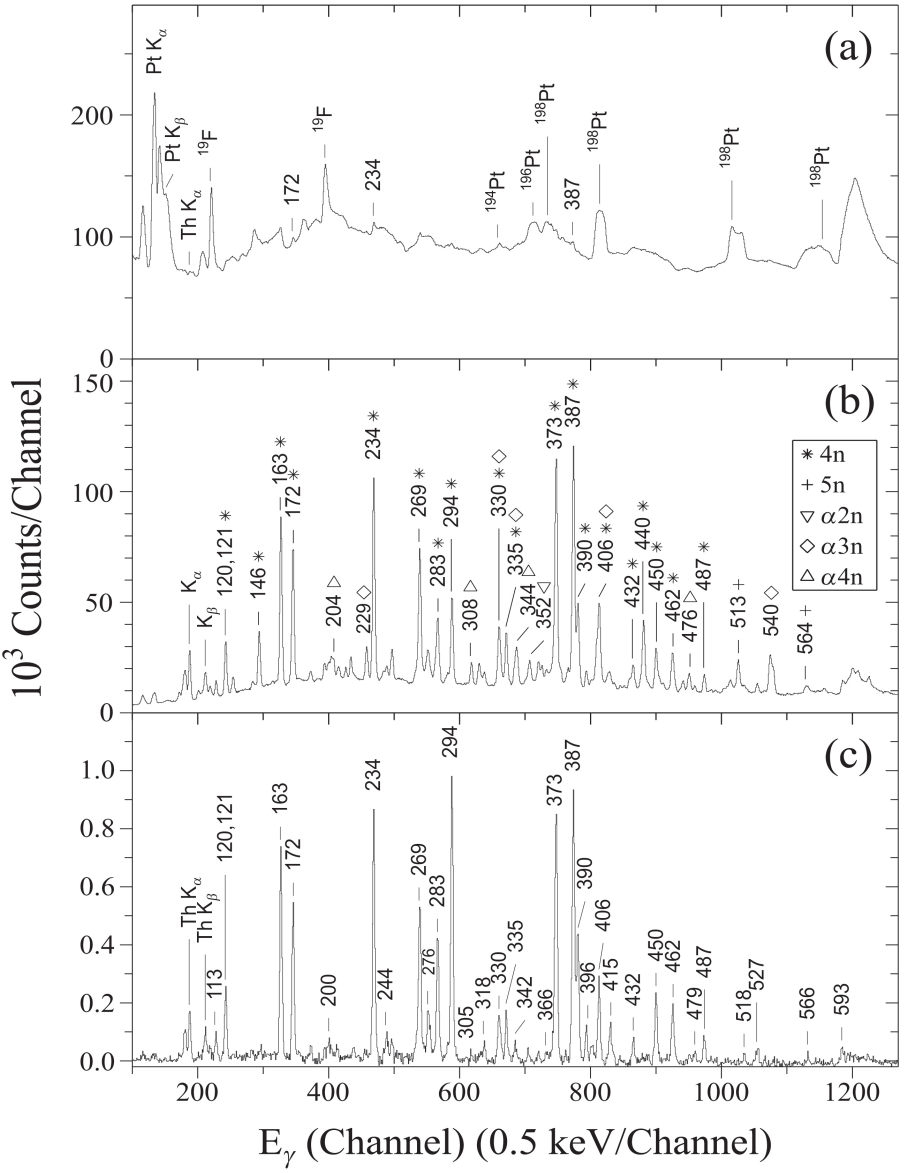

FIGURE 2. *Spectra for the ^{26}Mg on ^{198}Pt reaction at E_{lab} = 128 MeV. Shown are the "raw" spectrum for a fraction of the data (a), the projection of a residue-gated γ-γ coincidence matrix (b), and a residue- and γ-gated coincidence spectrum (c). The lines of interest are labeled by their energies in keV and, where appropriate, an additional symbol representing the evaporation channel. The figure is reproduced from Ref. [18].*

as the 4π array CHICO is operated on the basis of time-of-flight differences between reaction products [7].

The spectra of Ref. [20] are impressive examples for the Doppler correction of Gammasphere data assisted by an auxiliary detector. This results in the observation of new spectroscopic features and complex band interactions in ^{170}Er. Specifically, the so-called β-band, i.e., the excited level sequence with K quantum number and parity 0^+, is seen to survive at high spin. This is a remarkable result, since experimental evidence for the low-lying β-vibrational mode in deformed nuclei is sparse and often ambiguous.

The users of the Gretina-CHICO-2 combination have recently started with projectile multi-step Coulomb-excitation experiments at the CARIBU fission-fragment facility at Argonne's ATLAS accelerator [21]. One of the projects is measuring the strength of octupole collectivity in neutron-rich Ba nuclei, particularly $B(E3)$ values for transitions connecting low-lying rotational levels having opposite parity. This indicates a near-future direction for research in the broader region around ^{132}Sn.

Depending on the physics goal of the experiment, single-step Coulomb excitation may be the approach of choice. In this case, the final state of the transition being analyzed can only be populated directly, i.e., feeding from higher-lying levels is eliminated. A good example is the measurement of $B(E2)$ values for the $0^+ \rightarrow 2_1^+$ (first excited state) transitions in semi-magic ^{134}Te and neighboring isotopes [22]. (The setup was similar to those discussed above, but the CLARION array of 8 clover HPGe detectors was used [23].) Here, a light target (natural C) was in place, favoring a single-step excitation. This type of precision measurement works well for a systematic study of transition strengths in a larger set of nuclei and, thus, is particularly important in regions of the chart far from stability.

The principle of the experiment of Ref. [22] as well as the single-nucleon transfer studies discussed in the remainder of this

section is comparatively simple: only the target-like fragment (TLF) is detected, which is then correlated with the γ rays from the projectile-like fragment (PLF). Due to the strongly inverse-kinematic nature of the reactions, it is sufficient that the detector system covers laboratory angles in the forward hemisphere up to $\sim 70^\circ$ [9]; in these cases the detection efficiency is ~ 0.8. The PLF is focussed in a narrow cone around the beam axis, where it is allowed to escape detection.

In experiments with the CLARION-Hyball and Gammasphere-Micro-ball combinations, single-neutron states in the $N = 83$ nuclei ^{135}Te and ^{137}Xe, respectively, have been studied by inverse-kinematic reactions using ^{13}C and ^{9}Be targets [24]. The previously unknown $13/2^+_1$ levels are observed in both nuclei and their energies precisely measured. In, e.g., the ^{13}C(^{136}Xe,^{12}C)^{137}Xe case the level energy is 1753 keV. The present result provides the best empirical predictions for the neutron $0i_{13/2}$ state in the ^{132}Sn region, which is crucial for shell-model calculations. The result also highlights the usefulness of γ-spectroscopic information in transfer work and, in general, the selectivity of transfer reactions for certain states.

To elaborate on the latter aspect, a comparison of two versions of the ^{137}Xe level scheme is presented in Fig. 3. The version on the left is the level scheme of Ref. [24], whereas the scheme shown on the right is the result of a ^{248}Cm source experiment [25]. The left part of the figure is the significant one because of the presence of the $13/2^+$ level. However, the strong population of this level depends on the choice of the target. Following the ℓ- and j-selection rules for nucleon transfer discussed in Ch. 16 of Ref. [26], a $0i_{13/2}$, $j = \ell + 1/2$ state is preferably populated if the odd nucleon (of either the target or the beam nucleus) resides in a $j = \ell - 1/2$ orbital. Hence, by using a ^{13}C target, having a $0p_{1/2}$, $j = \ell - 1/2$ valence neutron, the change to the $0i_{13/2}$ orbital is favored over one to the candidate orbitals of $j = \ell - 1/2$ character. Conversely, using the same beam and a ^{9}Be target leads to a preference for the $j = \ell - 1/2$ orbitals in the odd-neutron

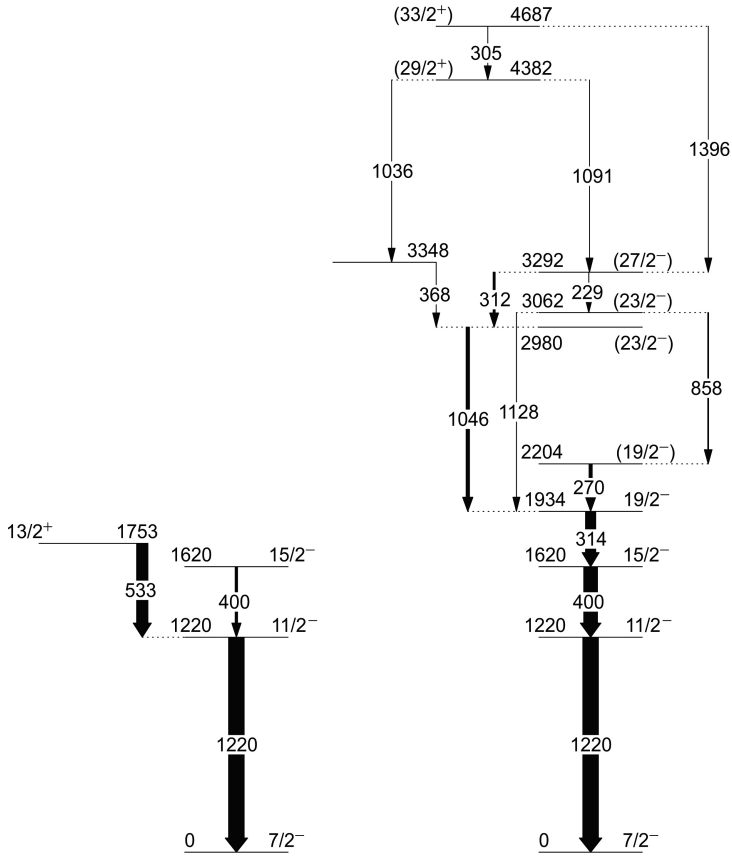

FIGURE 3. *The level scheme for ^{137}Xe, obtained with different population mechanisms. Shown are the results from a $^{13}C(^{136}Xe,^{12}C)$ reaction (left) and a ^{248}Cm spontaneous fission (right) measurement. The arrow widths are proportional to the γ-ray intensities. The 400- and 533-keV transitions (left) have a branching ratio $\sim 1:5$. The 533-keV transition is not observed in fission.*

reaction product. In conclusion, the choice of the target allows one to "dial" the state of interest.

From the previous discussion, it becomes obvious that the heavy-ion induced transfer reactions have been primarily used in a "neutron-adding" mode. In order to study the properties of proton states, e.g., $0g_{7/2}$ and $0h_{11/2}$ in the Sn region, one can use the same type of reactions, but with ^{10,11}B and ^{14}N (nitride) targets. Also

an option are "proton-removal" reactions such as ^{7}Li(A,^{8}Be)B. The issue is here to track these proton states in the neutron-rich regime, where the short-range proton-neutron interaction, as it is known in proton-rich and stable nuclei, will gradually change [13]. First proton-transfer measurements have been performed [27], in preparation for experiments with rare-isotope beams.

Another near-future task is the measurement of spectroscopic factors, a quantity that, in principle, provides the occupancy of the single-particle orbital of interest. The measurement is based on the cross section, σ, for populating the state, extracted from the center-of-mass PLF angular distribution, $\mathrm{d}\sigma/\mathrm{d}\Omega'_{PLF}(\theta'_{PLF})$; here Ω' is the solid angle. Although the angular distribution is a derived function, it is completely determined by the measured parameter θ_{TLF}, the groundstate-groundstate Q value, and the γ-ray spectroscopic information on a possible target excitation. Spectroscopic factors have not been measured with the Microball and the Hyball, because of the limited angular resolution of these detectors. They will be measured with the Phoswich Wall though.

Summary

A variety of examples for reaction-channel selected in-beam γ-ray spectroscopy on both sides of the β-stability valley and with both stable and rare-isotope heavy-ion beams have been discussed. The presentation outlines the experiments and justifies the choice of a particular detector setup. At the same time, the physics results are discussed in some detail. The setups and detection devices that have been presented, i.e., Gammasphere, Gretina, and their auxiliary particle detectors, are typical for the types of experiments discussed. Most of the statements made are, in principle, applicable to similar multi-detector setups used for γ-ray spectroscopy far from stability. Finally, the sequence in which the material has been presented follows the clear trend that the emphasis of nuclear-structure studies has shifted from proton- to neutron-rich nuclei. This concurs with the fact that neutron-rich nuclei have now a greater discovery potential.

The authors take the opportunity to acknowledge valuable discussions with J. M. Allmond, M. P. Carpenter, and C. Y. Wu during the preparation of the manuscript, technical support from J. M. Elson and J. E. Kinnison in many of the experiments discussed, and critical reading of the manuscript by K. W. Brown. Nuclear structure studies by the group at Washington University are, in part, supported by the US Department of Energy, Office of Nuclear Physics, Grant no. DE-FG02-88ER-40406.

References

[1] I. Y. Lee, Rep. Prog. Phys. **66**, 1095 (2003).
[2] H. Morinaga and T. Yamazaki, *In-beam gamma-ray spectroscopy* (North-Holland, 1976).
[3] D. Cline, Annu. Rev. Nucl. Part. Sci. **36**, 683 (1986).
[4] D. G. Sarantites et al., Nucl. Inst. Meth. **A 381**, 418 (1996).
[5] D. G. Sarantites et al., Nucl. Inst. Meth. **A 530**, 473 (2004).
[6] W. Reviol et al., Nucl. Inst. Meth. **A 541**, 478 (2005).
[7] M. W. Simon et al., Nucl. Inst. Meth. **A 452**, 205 (2000).
[8] C. Y. Wu, private communication (2014).
[9] D. G. Sarantites et al., Nucl. Inst. Meth. **A 790**, 42 (2015).
[10] A. Gallindo-Uribarri et al., AIP Conf. Proc. **1271**, 180 (2010).
[11] J. Erler et al., Nature **486**, 509 (2012).
[12] D. J. Morrissey and B. M. Sherrill, Phil. Trans. R. Soc. Lond. A **356**, 1985 (1998).
[13] D. F. Geesaman, C. K. Gelbke, R. V. F. Janssens, and B. M. Sherrill, Annu. Rev. Nucl. Part. Sci. **56**, 53 (2006).
[14] C. J. Chiara et al., Nucl. Inst. Meth. **A 523**, 641 (2004).
[15] C. J. Chiara et al., Phys. Rev. **C 67**, 041303(R) (2003).
[16] D. Rudolph et al., Phys. Rev. **C 82**, 054309 (2010).
[17] E. K. Johansson et al., Phys. Rev. **C 77**, 064316 (2008).
[18] W. Reviol et al., Phys. Rev. **C 74**, 044305 (2006).
[19] W. Reviol et al., Phys. Rev. **C 90**, 044318 (2014).

[20] C. Y. Wu et al., Phys. Rev. **C 61**, 21305 (2000).
[21] Argonne, (2014).
[22] D. C. Radford et al., Phys. Rev. Lett. **88**, 225201 (2002).
[23] C. J. Gross et al., Nucl. Inst. Meth. **A 450**, 12 (2000).
[24] J. M. Allmond et al., Phys. Rev. **C 86**, 031307 (2012).
[25] P. J. Daly et al., Phys. Rev. **C 59**, 3066 (1999).
[26] G. R. Satchler, *Direct nuclear reactions* (Clarendon Press, 1983).
[27] D. G. Sarantites et al., to be published (2015).